Material Science and Engineering International Research Journal
ISSN: 2997-6685|
Volume 12 Issue 4, October - December, 2024
Journal Homepage: https://ethanpublication.com/articles/index.php/E30
Official Journal of Ethan Publication

PREDICTING HEAT INPUT IN SHIELDED METAL ARC WELDING OF LOW CARBON STEEL PIPELINES USING BOX-BEHNKEN DESIGN

Chukwudi Emmanuel Nnaji and Abiola Samson Adekunle
Department of Mechanical Engineering, Faculty of Engineering, University of Port Harcourt, Rivers State, Nigeria
DOI: https://doi.org/10.5281/zenodo.17190812

Abstract
Heat input is an issue in a welding process of low-carbon-steel pipelines, leading to low heat input which cause lack of penetration and produce refined microstructure, and high heat input which give excess penetration, and cause coarse micro structure, reduce weld toughness and cause distortion. This study aims to produce mathematical model that will predict heat input in shielded metal arc welding of low-carbon steel pipelines, by means of a Box Behnken design of experiment with response surface technique using Minitab V15 and Sigma V15 softwares, utilized to optimize the variables. Heat input model was established to predict heat input as per welding parameters. The model displayed a good coefficient of determination R2 =0.9983, Adj R^2 = 0.9953, low standard errors = 0.0337 and PRESS = 0.0329. Hence, the model can predict the heat input using Box Behnken design technique, and model developed was quadratic of general form $yi \quad \beta iXi \quad \beta ijXiXj + \sum 3k = \beta kkX2k$. *These results were validated, comparing predicted values with the results of experimental and was achieved by means of generating a scatter diagram for the response (heat input). The result displayed there was a (good fit) between model predictions and experimental results. Furthermore, the response produced was influenced by voltage, welding current (XC), electrode temperature (XET) and preheat temperature (XPT). In accordance with relationship between input independent variables and dependent variables, it shows changing voltage, current (XC), electrode temperature (XET) and preheat temperature (XPT) resulted in significant impact in the response. However, the established model serves as a predictive tool for assessing the heat input in pipeline welding process.*

Keywords: *Heat input, Design of experiments, Response surface.*

INTRODUCTION

Pipelines are a cost-effective way to move gas and oil over long distances to many demand places, like refineries and flow stations [1] and [2]. Weld failures continue to be a recurring cause of pipeline failure, and weld quality can help prevent this. In a pipeline, the weld imperfections are therefore measured being the main source of stress. [3] and [4]. By applying heat to the right melting points and allowing the molten metals to form together, the welding process is a technique for joining two or several steel metal parts. The SMAW technique has the benefit of being the simplest of all arc welding procedures; the equipment is small and portable, and it is not as costly as others arc welding machines. Because a variety of electrodes are available to enable the welding of metal and their alloy, SMAW is a widely used welding procedure. The SMAW is widely used in almost every industry and fabrication department. Because of its inexpensiveness,

strong mechanical strength, abundant supply, higher melting temperatures, and range of mechanical qualities, steel, an iron carbon (Fe-C) alloy, is used
extensively in the material sectors [5-7]. It typically contains under 2.11 weight percent carbon. Carbon, stainless steel, alloy steel, and tool steels are among the different kinds of steel. The automobile and transportation sectors frequently use steel made of carbon. To produce the necessary item, this steel is often subjected to a welding procedure with varying heat input. The energy transmitted per length of weld is measured relative to the degree of heat input. One of the most important factors to consider while preparing welding process specifications (WPS) is heat input. The post weld heat treatment (PWHT) choice will be based on the values of the heat input. The amounts also affect the rate of cooling, which is one of the main determinants of the last metallurgical structures of the heat affected zone (HAZ) and weld. The width and sizes of HAZ grains are similarly influenced by heat input [8]. Furthermore, these parameters for welding are the primary determinants of welds joint embrittlement and Steel's strength and toughness are significantly impacted by microstructures [9,10]. Few microstructure studies on HAZ have been conducted based on the literature; nevertheless, there is a lack of specific studies on the coarse grain heat affected zone (CGHAZ) and fusion line (FL). Shielded metal arc welding (SMAW) and oxyacetylene welding (OAW) to examine the impact of heat input upon the mechanical property of steel with a low carbon content. On a particular size of steel with low carbon that was 10millimetres thick, two distinct edge prepares were examined using the following weld process parameters: two welding voltages of 100 and 220 Volts, different welding currents of 100 amperes, 120 amperes, and 150 amperes, and two mild-steel electrodes gauges of 10 mm and 12 mm. After testing the steel welded joint's hardness, tensile and impact strength, this was found that these properties decrease as the amount of heat used to the weld increases [11–13]. However, as the amount of heat input advances, so does the weldment's impact strength. In addition, it was found that, within similar conditions, V grooved edges preparation offers superior mechanical property to straight edges preparation. The microstructures of the weldments are significantly impacted by the rate of cooling in various media, according to micro structural analyses. The microstructures contained both pearlite & ferrite, while the ratio of ferrites to pearlites changed depending on the circumstances. Using various techniques, numerous attempts have been made to relate the process variables responsible for welded joint quality [14]. The methods of regression analysis, ANOVA, and response-surface technique [15–19] were used for this aim. In order to achieve an ideal welds quality, each model recommends selecting a specific amount of parameters for the process. Heat is needed during welding to melt the fillers materials and the surface, allowing for coalescence and the formation of a good, permanent joints after its solidification. As a result, heat input is crucial to weld fusion. Once more, the welding process current, welding voltage, and flame travel electrode speed all influence heat input. To give a exact heat input, these three parameters or variables must be chosen. The mechanism of transferring metal varies greatly for a given combination of welding current and voltage. Thus, the shapes of the welded bead is determined by the heat input and the metal transmission method. For a strong joint to develop in a welded joint, the weld-

bead shape must fully penetrate. [20, 21]. The potential variation between the welding cable tips and the melting welding pool's surface is known as voltage. It specifies the weld metal's reinforcement and the Fusion Zone's (FZ) forms. The penetration depth stays at its greatest at the ideal voltage, and the wider the weld, the flatter and less penetrating it is compared to the lower welding voltages. Heat input is an expression of the amount of energy transported per length of the welding joint [22, 23]. It's important because it affects the rate of cooling, which might have an impact on the metallurgy structure of weld metal (WM) and heat affected zone (HAZ) as well as their mechanical characteristics. Heat input is calculated using formula below.

$$H = \frac{60VI}{1000S}$$

V for voltage (V), I for current (A), S for travel speed (mm/s), and H for heat input (kJ/mm).

2.0 METHODS 2.1 Materials and Equipment

In this study ASTM A106 Gr B low carbon steel pipes of 6 inches' nominal pipe size with wall thickness 14.27mm were used as the base metal. The material was selected due to its wide range application such as Industrial plants, power plants, refineries and chemical plants. The chemical compositions are analysed by Optical emission spectrometers as shown in Figure 1 (a&b). The chemical analysis (PMI-Optical Emission spectrometers) was performed to ascertain the chemical composition of the selected material.

Figure 1: (a) Optical Emission Spectrometers machine and (b) Certificate of chemical analysis.

Table 1: Chemical-composition of base metal (BM) (wt%)

Element	C	Si	Mn	P	S	Cu	Al	Cr	Mo	Ni	V	Ti
	0.122	0.236	1.306	0.011	0.005	0.005	0.018	0.144	0.066	0.038	<0.001	0.003
	0.133	0.243	1.347	0.012	0.004	0.006	0.018	0.156	0.07	0.043	<0.001	0.003
	0.132	0.242	1.325	0.01	0.005	0.006	0.018	0.142	0.066	0.038	<0.001	0.003

Average	**C**	**Si**	**Mn**	**P**	**S**	**Cu**	**Al**	**Cr**	**Mo**	**Ni**	**V**	**Ti**
Wt%	0.129	0.24	1.326	0.011	0.005	0.006	0.018	0.147	0.067	0.04	<0.001	0.003

Element	**Nb**	**Co**	**W**	**Pb**	**B**	**As**	**Bi**	**N2**	**Sn**	**Sb**	**Ca**	**CE**
	0.025	0.002	<0.001	0.006	<0.0002	<0.001	0.004	0.01	0.004	<0.001	0.0065	0.38
	0.03	0.003	<0.001	0.006	<0.0002	<0.001	0.003	0.002	0.003	<0.001	0.0052	0.42
	0.026	<0.001	<0.001	0.006	<0.0002	<0.001	0.003	<0.001	0.004	<0.001	0.0066	0.4
Average	**Nb**	**Co**	**W**	**Pb**	**B**	**As**	**Bi**	**N2**	**Sn**	**Sb**	**Ca**	**CE**
Wt%	0.027	0.002	<0.001	0.006	<0.0002	<0.001	0.003	0.004	0.004	<0.001	0.0061	0.4

Manganese (Mn), lead (Pb), boron (B), arsenic (As), bismuth (Bi), molybdenum (Mo), chromium (Cr), aluminum (Al), nickel (Ni), titanium (Ti), vanadium (V), copper (Cu), sulfur (S), Tin (Sn), Antimony (Sb), phosphorus (P), and nitrogen (N).

ESAB 55.00 of low hydrogen electrode E7018 was utilized for root-pass, hot-pass, fillings and capping's as a consumable as presented in Table 2

Table 2: Experimental Electrode

Manufacturer	Classification	Group	Sizes	Batch No
Esab-55.00	AWS-E7018-1H4R	A5.1	2.5	EC229532566Rev0
Esab-55.00	AWS-E7018-1H4R	A5.1	3.2	EC24826988Rev0

Table 3:Base Metal Identification

Pipe identification	Thickness (mm)	Nominal Pipe size	Material Type
Low Carbon Steel	14.27mm	6''Sch120	ASTM-A106 GR-B

Material Science and Engineering International Research Journal
ISSN: 2997-6685|
Volume 12 Issue 4, October - December, 2024
Journal Homepage: https://ethanpublication.com/articles/index.php/E30
Official Journal of Ethan Publication

Super Arc – 4000 electrical welding machines were used in this study as shown in Figure 2. It is powerful machine designed for heavy duty welding application.

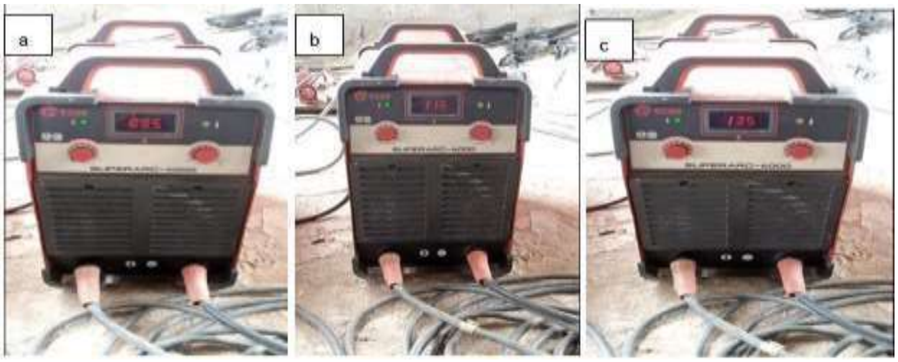

Figure 2: Photograph of Electrical welding machine (Super Arc 4000) (a) 095A (b) 115A (c) 135A.

2.2 Methods

This research, the welding process of SMAW was used to weld the base metal by utilized E7018 electrode, 2.5mm diameter for the root-pass and 3.2mm diameter for hot-pass, filling and capping. The weld parameters that were used in this research was maintained and steps of this experimental work has been considered. The test pipe coupon thickness of 14.27mm and longitudinally cut with single-v-joint, prepared with bevel-angle between 50°- 60°, and with root-gap equal to 3mm and root-face equal to 2 mm. The weld position was 45-degree angle (6G POSITON) as seen in Figure 3-a, the test pipe coupons were welded in accordance with the BBD Experimental design matrix as indicated in Table 6 by qualified welder and also qualified to weld the same process (SMAW).The fifteen coupons were marked as W01, W02 to W15, each weld joint were welded at different temperature 100°C, 175°C, and 250°C. Table 6 displayed welding (input) variables for each weld that comprise the inter-pass temperature range, welding amperage and voltage that was used for samples W01, W02, to W15.Weld direction (Vertical-uphill) and bead sequences were maintained, and Figure 3 shows test coupon before and after welding. Prior to start, it was preheated to dry of the moisture, because; to reduce rate of cracking, improve weld penetration, reduce distortion and improve quality of weld by reduce porosity. Inter pass temperature, welding currents and voltages were taken on every stages. Immediately after the completion of the welding operation, the weld beads and weld toe at the capping surface were cleaned with wire brush.

Material Science and Engineering International Research Journal
ISSN: 2997-6685|
Volume 12 Issue 4, October - December, 2024
Journal Homepage: https://ethanpublication.com/articles/index.php/E30
Official Journal of Ethan Publication

Figure 3: Photograph of test coupon (a) before and (b) Photograph of #15 welded pipes

The experiment was designed and carried out to forecast the welding heat input in welded carbon steel pipeline and to optimize the parameters using the Box-Behnken design of experiments in conjunction with the Response-surface approach utilizing Minitab V 15.0 and Sigmal plot V15.0 softwares. 15 experimental runs with one repetition each were produced by using three parameters in the BBD (3^3): preheat temperature (X_{PT}), current (X_C), and electrode temperature (X_{ET}) at three levels each [18]. The response surface approach is a useful statistical and mathematical technique for modeling and forecasting outcomes influenced by a variety of variable inputs in order to improve responses [24]. The response surface method identifies a relationship among one or more measure response and the significance that controls the input parameters [27]. If each of the predictors variables can be determined as well as repeated with negligible errors, then the response surface can be defined as follows: y=f (X_1, X_2, ...X k), where k is the number of (predictor) independent variables. In order to maximize response "y," it is necessary to determine an appropriate estimation for the actual functional relationship between each predictor variable and the response-surface. Typically, a 2nd order Polynomial Equation (1) is used in this method.

$$y = b_0 + \Sigma b_i X_i + \Sigma b_{ij} X_i X_j + \Sigma b_{ii} X^2_{ii} + \mathcal{E} \qquad (1)$$

In a BBD, the actual levels of the factors in the experiment are represented by the coded values (-1, 0, and +1), which are standardized values. Using equations (1) through (4), the standardization process reduces the weight of each component to standard or normalized values of -1, 0, and +1. [24] and [25].

$$X_C = \frac{C_c - 115}{20} \qquad (2)$$

$$X_{ET} = \frac{E_{Tc} - 150}{50} \qquad (3)$$

$$X_{PT} = \frac{P_{Tc} - 175}{75} \qquad (4)$$

where

X_C: Current (A)

X_{ET}: Electrode Temperature (°C)

X_{PT}: Preheat Temperature (°C)

C_C : Current at centre level

E_{TC} : Electrode temperature at centre level

P_{PT} : Preheat temperature at centre level

Material Science and Engineering International Research Journal
ISSN: 2997-6685|
Volume 12 Issue 4, October - December, 2024
Journal Homepage: https://ethanpublication.com/articles/index.php/E30
Official Journal of Ethan Publication

The data required to designed and carry out the experiments used for heat input prediction was shown in Table 4, which also produced the design experiment matrix shown in Table 5.

Table 4: Coded values and Levels of three Factors for BBD

Factors	Unit	Symbols	Coded values and Levels		
			-1	0	1
Current	A	X_C	95	115	135
Electrode Temperature	°C	X_{ET}	100	150	200
Preheat Temperature	°C	X_{PT}	100	175	250

Table 5: Experimental design matrix for Three Factor BBD and coded values

Run order	Standard order	Current (A)	Electrode temperature **(°C)**	Preheat temperature **(°C)**	X_C	X_{ET}	X_{PT}
6	1	95	100	175	-1	-1	0
13	2	135	100	175	1	-1	0
11	3	95	200	175	-1	1	0
5	4	135	200	175	1	1	0
10	5	115	100	100	0	-1	-1
1	6	115	200	100	0	1	-1
8	7	115	100	250	0	-1	1
4	8	115	200	250	0	1	1
9	9	95	150	100	-1	0	-1
3	10	135	150	100	1	0	-1
14	11	95	150	250	-1	0	1
12	12	135	150	250	1	0	1
2	13	115	150	175	0	0	0
15	14	115	150	175	0	0	0
7	15	115	150	175	0	0	0

Table 6: Parameters used during welding operation

Material Science and Engineering International Research Journal
ISSN: 2997-6685|
Volume 12 Issue 4, October - December, 2024
Journal Homepage: https://ethanpublication.com/articles/index.php/E30
Official Journal of Ethan Publication

Sample	Preheat temperature **(°C)**	Root pass (Amps)	Hot pass (Amps)	1st Filling (Amps)	2nd Filling (Amps)	Capping (Amps)	Voltage (Volts)
W01	175	95	95	95	95	95	27
W02	175	135	135	135	135	135	27
W03	175	95	95	95	95	95	26
W04	175	135	135	135	135	135	24
W05	100	115	115	115	115	115	26
W06	100	115	115	115	115	115	27
W07	250	115	115	115	115	115	24
W08	250	115	115	115	115	115	24
W09	100	95	95	95	95	95	26
W10	100	135	135	135	135	135	27

Sample	Preheat temperature **(°C)**	Root pass (Amps)	Hot pass (Amps)	1st Filling (Amps)	2nd Filling (Amps)	Capping (Amps)	Voltage (Volts)
W11	250	95	95	95	95	95	24
W12	250	135	135	135	135	135	26
W13	175	115	115	115	115	115	27
W14	175	115	115	115	115	115	24
W15	175	115	115	115	115	115	26

Note; Direct current electronegative(DC-) was used for the root pass and Direct current electropositive(DC+) was used for hot pass, filling and capping.

The R^2 result typically indicates the amount of variation around the average that the model can explain. The Adjusted R^2 shows how much of the variance around the mean is addressed by a certain model when the number of term in the model takes into consideration. The adjusted R^2 reduces as the number of term increases if the additional terms for the mathematical model do not increase its value. The R^2 and related

Adjusted R^2 number should be closer to one (1), per [24] and [25]. When the chosen model is able to explain each of the variations in the observed value, the value for 1 indicates the optimum situation [24] and [25]. The PRESS statistics compute the amount of variance in the new data that the model will account for, and the Predicted R^2 show how well the model match the overall data; the closer the predicted R^2 is to 1, the more accurate the predicted value. The purpose of this study is to develop a model for forecasting the welding heat input in a welded pipeline. Moreover, the studies were conducted using a three-factor Box-Behnken Design. One of the most often used RSM designs, the Box Behnken design was used in this study because it is robustness and less expensive than other DOEs such full factorial (FF), central composite design (CCD), and central composite design-Face (CCF). [18]

3.0 RESULTS AND DISCUSSIONS 3.1 Electrode Travel speed and Heat Inputs

The different Electrode travel speeds and heat inputs for root pass, hot pass, filling and capping

Table 7: Welding control parameter

Test run number	**Voltage (V)**	**Current (A)**	**Length (mm)**	**Time (Sec)**	**Travel Speed (mm/sec)**	**Heat input (KJ/mm)**
W01	27	95	548	284.333	1.927320649	1.33054788
W02	27	135	549	395.333	1.388703491	2.624734098
W03	26	95	548	297.667	1.840990065	1.34012749
W04	24	135	547	436.667	1.252681986	2.587341664
W05	26	115	549	344.333	1.597292439	1.871191212
W06	27	115	548	316.667	1.730530155	1.796421825
W07	24	115	547	367.667	1.49048296	1.852751825
W08	24	115	549	358.667	1.530687679	1.806732969
W09	26	95	548	289.000	1.896208907	1.302309489
W10	27	135	549	391.00	1.404116563	2.595733607
Test run number	**Voltage (V)**	**Current (A)**	**Length (mm)**	**Time (Sec)**	**Travel Speed (mm/sec)**	**Heat input (KJ/mm)**
W11	24	95	548	312.333	1.754563688	1.299589051
W12	26	135	549	407.000	1.348899778	2.602131148

Material Science and Engineering International Research Journal
ISSN: 2997-6685|
Volume 12 Issue 4, October - December, 2024
Journal Homepage: https://ethanpublication.com/articles/index.php/E30
Official Journal of Ethan Publication

W13	27	115	548	316.667	1.730576031	1.79531825
W14	24	115	549	355.333	1.545063584	1.786345228
W15	26	115	548	342.667	1.599233873	1.869849367

The Table 8 of the quadratic model for the heat input presented a good coefficient of determination (R^2) as low-standard error and predicted-residual-error-sum-of-square (PRESS).

In the present case, the standard error was small and the coefficient of determination (R^2), Adjusted (R^2) and predicted (R^2) are close to 1 which show that, the established mathematical model is perfect accurate. A small values are necessary for the PRESS statistic to provide a measures of the degree to which a given model suits every possible design points, which was the cases in the present study.

It is evident from the results shown in Table 9 that the standard error of intercept, linear, interaction and quadratic terms are small, which is another goodness-of fit measure that shows the precision of the regression analysis. In case of the heat input model, the main effects are voltage, current(X_C), preheat temperature(X_{PT}) and electrode temperature(X_{ET}) and all interaction terms also effect the model. The second order effect of current(X^2_C), preheat temperature(X^2_{PT}) and preheat temperature(X^2_{PT}) also contribute to the model but current(X^2_C) is more significant. However, current(X_C) is most significant factor associated with the heat input model. which are all in agreement with findings of [18,24,25,26].

The F-value of a mathematical model terms are used to compare the term-variance against the residual-variance of the mathematical-model and test the model's overall relevance. It can be stated mathematically as a ratio between the residual's mean square to the term's mean square. For a given term-model, a probability values that corresponds to the F-value is the Pvalue (Prob.> F). Typically, any term with a probability values that are below 0.05 (5%), is not-significant or a value above 0.05, is regarded as having a significant effect; however, in this investigation, the value was found to be 0.00000214 (0.000214%). In general, the model is a good one. Thus, the Value of prob.> F is less-than (0.05), then is significant.

The results of the predicted and experimental-values of heat-input are displayed in Table 10. For every response, an aggregate of 15 experimental final results had been acquired. The values acquired for the results from the experiment along with the values predicted through the regression equation are shown to be closed together for all responses taken into consideration. This shows that the mathematical model established is in accordance with is valid. By contrasting them against the actual-experimental-results, the regression model's predicted results for the responses which confirmed the validation. To do this, a parity-plot (scatter diagram) was generated and Figure 4 displays the result. The fact that the plot's data points are nearly aligned with the diagonal axis indicates that the mathematical model predictions and the results of experimentation fit each other effectively [18,26].

Table 8: Summary of model fit results of Heat input model.

Source	Multiple R	R^2	Adjusted R^2	Predicted R^2	Standard Error	PRESS	Observations

Model	0.992	0.9983	0.9953	0.9902	0.0337	0.0329	15

Table 9: Coefficients and Standard error for the Heat input design model

Term	Coefficients	Standard Error	p-value	Remarks
Intercept	1.8171	0.0194	0.000	
X_C	0.6422	0.0119	0.000	Significant
X_{ET}	-0.0186	0.0119	0.179	Not-Significant
X_{PT}	-0.0005	0.0119	0.969	Not-Significant
$X_C X_{ET}$	-0.0117	0.0168	0.516	Not-Significant
$X_C X_{PT}$	0.0023	0.0168	0.898	Not-Significant
$X_{ET} X_{PT}$	0.0072	0.0168	0.687	Not-Significant
X_{2C}	0.1358	0.0175	0.001	Significant
X_{2ET}	0.0177	0.0175	0.358	Not-Significant
X_{2PT}	-0.0030	0.0175	0.872	Not-Significant

Table 10: Experimental and predicted result of Heat input design model

Standard order	Factors			Heat input Response		
	Current (A)	Electrode Temperature (°C)	Preheat Temperature (°C)	Actual experiment (mm)	Predicted (mm)	Percentage Error(%)
1	95	100	175	1.3305	1.3353	**-0.36%**
2	135	100	175	2.6247	2.6431	**-0.70%**
3	95	200	175	1.3401	1.3217	**1.39%**
4	135	200	175	2.5873	2.5825	**0.19%**
5	115	100	100	1.8712	1.8582	**0.70%**
6	115	200	100	1.7964	1.8066	**-0.56%**
7	115	100	250	1.8530	1.8428	**0.55%**
8	115	200	250	1.8070	1.8200	**-0.71%**
9	95	150	100	1.3023	1.3105	**-0.63%**
10	135	150	100	2.5957	2.5903	**0.21%**
11	95	150	250	1.2996	1.3050	**-0.41%**
12	135	150	250	2.6021	2.5939	**0.32%**

13	115	150	175	1.7953	1.8171	**-1.20%**
14	115	150	175	1.7863	1.8171	**-1.70%**
15	115	150	175	1.8698	1.8171	**2.90%**

Heat input model

$$Heat\ input\ (H) = 1.8171 + 0.6422X_C - 0.0186X_{ET} - 0.0005X_{PT} - 0.0117X_CX_{ET} + 0.0023X_CX_{PT} + 0.0072X_{ET}X_{PT} + 0.1358X^2{}_C + 0.0177X^2{}_{ET} - 0.003X^2{}_{PT} \quad (5)$$

The experimental conditions, actual experimental values, and prediction error percentages were shown in Table 10. The relationship within the actual and predicted values of heat input, is displayed in Figure 4. Since the residuals in each response's prediction are very small and usually fall near the diagonal axis, that shows the established model is appropriate. According to [18] that the minimum error percentage for actual experimental and predicted values using Box-Behnken design around 5% or less. less than 5% is considered excellent agreement between actual and predicted values, while 5-10% is considered as good agreement and 1015% is considered as fair agreement. Therefore, given that the maximum prediction error percentage becomes 2.90%, indicating that they are in good-agreement, it is clear that the mathematical models can accurately represent responses throughout each range taken into consideration.

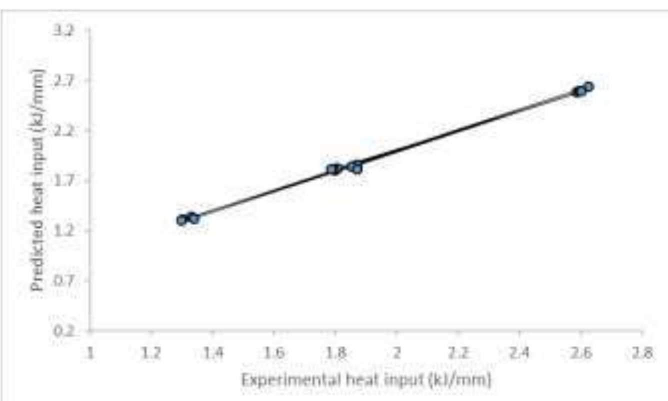

Figure 4: Scatter diagrams for Heat input

It is obvious from Figure 6 that, the parameters have effect on the heat input, but current (X_C) most significantly influence the response and preheat temperature (X_{PT}) and electrode temperature (X_{ET}) have no significant influence. As the voltage and current (X_C) increasing the heat input increasing, whereas the relationship amongst the preheat temperature (X_{PT}), and the heat-input is in reverse. Meaning that as preheat temperature (X_{PT}) decrease, the heat input increase slightly. Also as electrode temperature (X_{ET}) increase heat input reduce slightly. Figure 5 and Figure 6 shows that the predictors affect the response, but the current (X_C) is the most factor that influence the heat input and the electrode temperature (X_{ET}) and preheat temperature (X_{PT}) have no significant effect. However, as the current (X_C) increase from 95A to 115A, the heat input increase significantly, and as the electrode temperature (X_{ET}) and preheat temperature (X_{PT}) increases, the heat input reduce slightly. Nevertheless, increase the current (X_C) and decrease the electrode temperature (X_{ET}) and preheat temperature (X_{PT}) resulting to increase in heat input. Figure 6 displaced that, the invariable preheat-temperature(X_{PT}) and electrode-temperature (X_{ET}) have no significant effect on the heat input but current (X_C) has significant effect. However, an increase in voltage, and current (X_C) increase the heat input. When process factors; electrode temperature (X_{ET}) and preheat temperature (X_{PT}) increase, the heat input decreases and when the factors decrease, the heat input increase. The optimization results for the heat input shows that, current (X_C) at 95A and electrode temperature (X_{ET}) at this point 100 ^oC and preheat temperature (X_{PT}) at 100 ^oC lead to maximum heat input of 1.3423kJ/mm, and current (X_C) at 95A and electrode temperature (X_{ET}) at 150 ^oC and preheat temperature (X_{PT}) at 250 ^oC resulted in minimum heat input of 1.3049kJ/mm. Also, at current(X_C) 115A and electrode temperature (X_{ET}) at 100 ^oC and preheat temperature (X_{PT}) at 100 ^oC, maximum heat input 1.8581 kJ/mm was gotten, but current (X_C) at 115A and electrode temperature (X_{ET}) at 190 ^oC and preheat temperature (X_{PT}) at 100 ^oC lead to minimum heat-input 1.8053kJ/mm. For current (X_C) at 135A and electrode temperature (X_{ET}) at 100 ^oC and preheat temperature (X_{PT}) at 100^oC, resulted in maximum heat input of 2.6455kJ/mm, nonetheless current (X_C) at 135A and electrode temperature (X_{ET}) at 200 ^oC and preheat temperature (X_{PT}) at 100 ^oC gives minimum heat input of 2.5705kJ/mm.

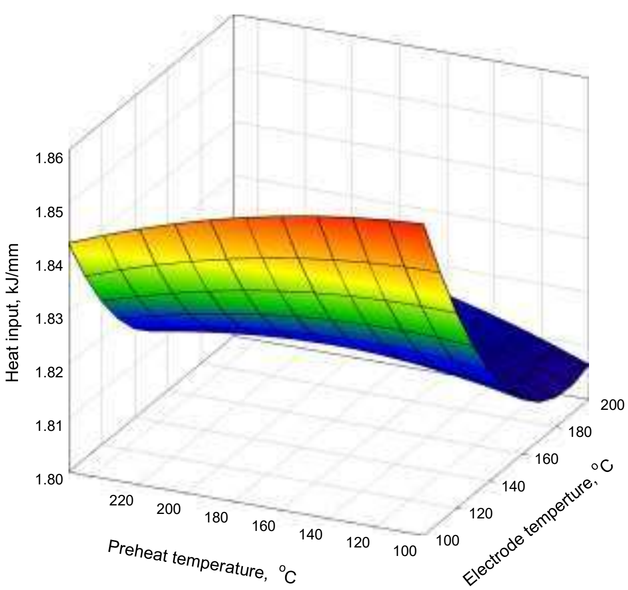

Figure 5: Response surface of heat input at Current (X_C) equal to 115A

3D Graph 15

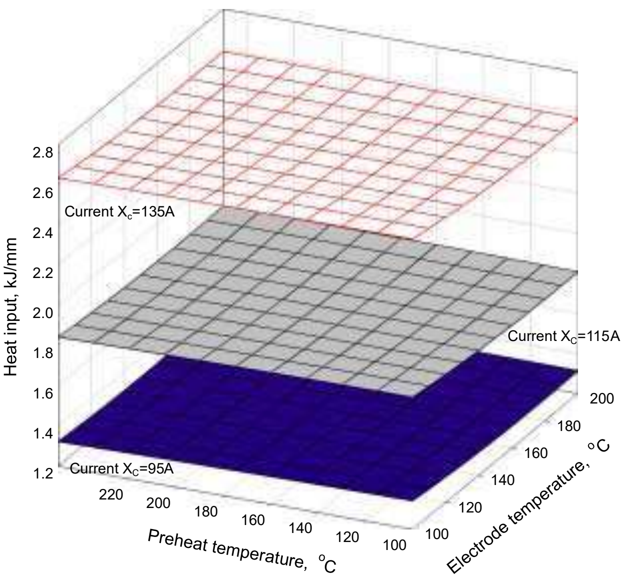

Figure 6: Response surface of heat input at different current (X_C) of 95A, 115A and 135A.

4.0 CONCLUSION

The Box-Behnken design technique was successfully used in this study to predict the heat input in the welding process. By comparing outcomes that were predicted by the mathematic model with the real experimental results, the evaluation of the predictive developed mathematical model for responses was assessed. Coefficient of determination (R^2), adjusted coefficients of determination (value of adjusted R^2), and standard error were used to assess the (degree of fit). The results showed that the mathematical model fits the heat input under consideration. The developed mathematical model demonstrated little standard errors (0.0337, PRESS = 0.0329) and an excellent coefficient of determination (R^2 = 0.9983 & adjusted R^2 = 0.9953). This verified that the experimental approach of heat input using the Box-Behnken design technique would be capable to estimate the heat input using the mathematical model.

By comparing the predicted result with the experimental outcome, the results' validity was assessed. This was therefore accomplished by creating a scatter diagram demonstrating the responses, and the results showed that the model's prediction with the actual experimental results fit each other effectively. Additionally, the voltage, welding process currents (X_C), electrodes temperature (X_{ET}), and preheat temperatures (X_{PT}) all had a full impact on the resulting heat input produced. The response heat input was significantly impacted by changes in voltage, welding current (X_C), preheat temperature (X_{PT}), and electrode temperature (X_{ET}), according to the correlation between input variables that are independent along with dependent variables. However, the real experimental values are fitted to this model, and the results have been validated by comparing the experimental results with the predicted values. Additionally, optimization was done to determine the maximum and minimum heat input.

REFERENCES

Hansen, M.E. and Dursteler, E. “Pipeline, rail & trucks: Economic, environmental, and safety impacts of transporting oil and gas in the U.S, Strata” 2017, 1–6.

C.F. Mason, A comparison of the risk of transporting crude oil: Rail vs. pipeline, IAEE Energy Forum. (2018) 5–7.

Vervynckt, S. Verbeken, K., Lopez, B. and Jonas, J.J, “Modern HSLA steels and role of non-recrystallisation temperature,” International Materials Reviews. 57, 2012, 187– 207.

Baker, T.N. “Microalloyed steels, Ironmaking and Steelmaking” 43, 2016, 264–307.

M. Morcillo, D. De la Fuente, I. Díaz and H. Cano.2011. Atmospheric corrosion of mild steel. Revista de Metalurgia. 47(5): 426-444.

Tkalcec I. 2004. Mechanical properties and microstructure of high carbon steel. Phd thesis, University of Zagreb, Croatia.

Totten G. E. 2006. Steel heat treatment handbook. 2nd Ed. CRC Press, Florida, USA.

E. Ranjbarnodeh, S. Weis, S. Hanke and A. Fischer. 2012. EBSD characterization of the effect of welding parameters on HAZ of AISI409. Journal of Mining and Metallurgy. 48(1): 115-121.

N. S. M. Nasir, M. K. A. A. Razab, S. Mamat and M. I. Ahmad. 2016. Review on welding residual stress. ARPN Journal of Engineering and Applied Sciences. 11(9): 6166-6175.

Popović O., Prokić-Cvetković R., Burzić M. and Milutinović Z. 2010. The effect of heat input on the weld metal toughness of surface welded joint. In: 14th International Research/Expert Conference: Trends in the Development of Machinery and Associated Technology. pp. 11-18.

M. A. Bodude1, I. Momohjimoh. "Studies on Effects of Welding Parameters on the Mechanical Properties of Welded Low-Carbon Steel", Journal of Minerals and Materials Characterization and Engineering, 2015, 3, 142-153 May 2015.

Lee, C. S., Chandel, R. S., and Seow, H. P. “Effect of welding parameters on the size of heat affected zone of submerged arc welding”, Materials and Manufacturing Processes, 15(5), 2000, 649-666.

[1] M. A. Gaodi and D. Sangotra, ``A review paper on effect of varying welding heat inputs on microstructure, mechanical properties and corrosion behaviours of ferritic stainless steel & mild steel,'' International Journal of Modelling Engi- neering Resolution, vol. 4, no. 1, pp. 105-109, 2014.

K.Y. Benyounis, A.G. Olabi, Optimization of different weldingprocesses using statistical and numerical approaches—a reference guide. Adv. Eng. Softw. 39, 483–496 (2008)

K.S. Prasad, C.S. Rao, D.N. Rao, Review on application of response surface method based design of experiments to welding processes. J. Manuf. Sci. Prod. 12, 17–24 (2012)

P. Sreeraj, T. Kannan, S. Maji, Prediction and optimization ofweld bead geometry in gas metal arc welding process using RSM and Fimincon. J. Mech. Eng. Res. 5(8), 154– 165 (2013) Antony, J. "Design of experiments for engineers and scientists", Elsevier, 2003.

Box, G. E. P. and Behnken, D. W. "Some new three level designs for the study of quantitative variables", Technometrics, Vol. 2, n., 4, pp. 1960, 455-475.

Chatterjee, S. and Price, B. "Regression analysis by example", 2nd Ed., Wiley and Sons, Inc., 1977, pp. 200-202.

Agilan, M., Venkateswaran, T., Sivakumar, D. and Pant, B. "Effect of heat input on microstructure and mechanical properties of inconel-718 EB Welds", Procedia Materials Science, 5, 2014, 656-662.

Dutta, J., and Narendranath, S. "Estimation of cooling rate and its effect on temperature dependent properties in welded high carbon steel joints", 2014.

Thornton, C. E., and Webster, D. J. (1990). Progress in the use of metal powder additions for the welding of offshore structures. In Proceeding of the Ninth International Conference on offshore mechanics and arctic Engineering. 3, 399-408).

M. A. Gaodi and D. Sangotra, ``A review paper on effect of varying welding heat inputs on microstructure, mechanical properties and corrosion behaviours of ferritic stainless steel & mild steel,'' International Journal of Modelling Engi- neering Resolution, vol. 4, no. 1, pp. 105-109, 2014.

Montgomery, D. C. "Design and Analysis of Experiments", 2nd Edition, John Wiley & Sons, New York, 1984.

Hicks, C. R. "Fundamental concepts in the design of experiments", 4th Ed., Saunders College Publishing, 1993.

Pekka, N. "Designed a predictive model for the prevention of weld metal hydrogen cracking in high strength multipass welds", Department of Mechanical Engineering, University of Oulu, 2003.

Khuri A. I. and Cornell, J. A. "Response Surfaces Design and Analysis", 2nd Edition, Marcel Dekker, New York, 1996.